

Highly Selective Oxygen Transport through a Cobalt Porphyrin Liquid Membrane

Xue-Si Chen, Hiroyuki Nishide,* Kenichi Oyaizu, and Eishun Tsuchida*,†

Department of Polymer Chemistry, Waseda University, Tokyo 169, Japan

Received: March 28, 1997; In Final Form: April 26, 1997[®]

The facilitated transport of oxygen in a liquid membrane containing [*meso*- $\alpha,\alpha,\alpha,\alpha$ -tetrakis(*o*-pivalamidophenyl)porphyrinatocobalt(II)]–laurylimidazole (CoP) as an oxygen carrier leads to high permeability and permselectivity of oxygen against nitrogen. The oxygen permeation was properly analyzed by a dual-mode model and using the oxygen-binding constants spectroscopically determined, to give permeation parameters of the membrane such as the diffusion coefficient (D_{CoP}) of the CoP mobile carrier and the physical diffusion coefficient of oxygen. D_{CoP} was in accordance with that electrochemically determined. The facilitated permeation was represented by the product of the CoP concentration and D_{CoP} in the membrane solution. D_{CoP} decreased with solution viscosity and increased with the measured temperature. High oxygen permeability ($10^{-7} \text{ cm}^3(\text{STP}) \text{ cm cm}^{-2} \text{ s}^{-1} \text{ cmHg}^{-1}$) was observed, *e.g.* for the membrane of the 31 wt % CoP methylanisole solution at 10 °C, where the facilitation factor and the oxygen/nitrogen permselectivity were over 20 and 40, respectively.

Introduction

A liquid membrane, which is prepared by immersing a microporous membrane into a solution of a carrier molecule, often displays carrier-mediated or facilitated transport. The carrier reversibly reacts with a specific component to form an adduct, thereby increasing the transport rate of this component relative to other components in the feed stream.^{1,2} The liquid membrane holding the carrier for facilitated transport improves both the selectivity and flux of the specific component.

The first demonstration of the facilitated transport was made by a membrane holding an aqueous hemoglobin solution in which hemoglobin specifically binds oxygen from air and enhances by several times the oxygen permeability through the membrane.³ The authors followed and analyzed this facilitated transport of oxygen with a liquid membrane of aqueous bovine hemoglobin solution.⁴ The hemoglobin-mediated and -facilitated transport of oxygen was properly analyzed with a dual-mode transport model. However, hemoglobin is unstable in an *ex vivo* solution and is too bulky (mol wt 64 500) as a carrier of the small oxygen molecule.

The facilitated transport of oxygen with liquid membranes for oxygen/nitrogen separation from air has been established and much improved by the group at Bend Research Inc.⁵ They used a series of cobalt Schiff-base complexes as the oxygen carrier in liquid membranes. A typical example is a microporous membrane containing a butyrolactone solution of [*N,N'*-bis(salicylidene)-*n*-propyldipropylenetriamine]cobalt, at –10 °C, which exhibited an oxygen/nitrogen selectivity of 20. The membrane yielded *ca.* 80% oxygen-enriched air through air permeation at –10 °C. However, the operation of such membranes was limited at low temperature, because the low-temperature operation enhances the oxygen-adduct formation of the carrier and suppresses irreversible oxidation of the carrier through the repeated oxy–deoxy cycle.⁵

The oxygen flux and permselectivity in the liquid membrane for facilitated transport are related to the critical fundamental parameters of the membrane, that is, the concentration of the carrier solubilized in the liquid medium, the diffusivity of the

carrier in the membrane, the oxygen-binding affinity and kinetics of the carrier, and so on.^{1,2,5} For example, the facilitated transport increased with the carrier concentration in the liquid medium up to the optimum concentration, simply because there was more carrier available for oxygen transport. But the solution viscosity of the liquid medium significantly increased with the carrier concentration and the diffusivity of the relatively large oxygen carrier fell, which tremendously retards the facilitated transport. However, the diffusion coefficient of the synthetic carrier such as the cobalt complex has not yet been estimated in the facilitated oxygen transport or air separation membrane, which is one of the significant liquid membranes. The authors analyzed in a previous paper⁴ the facilitated oxygen transport through a hemoglobin liquid membrane using a dual-mode transport model to give the diffusion coefficient of the mobile carrier, hemoglobin, and the solution–diffusion coefficient of oxygen in the liquid membrane.

The authors have been studying metalloporphyrins as an efficient oxygen carrier⁶ and are applying them to an artificial red cell,⁷ an oxygen adsorbent,⁸ and oxygen-permselective solid membranes.⁹ In this paper, a cobaltporphyrin derivative has been for the first time successfully applied as an oxygen carrier to a liquid membrane. Advantages of the cobalt porphyrin as the carrier of a liquid membrane are as follows: (i) rapid oxygen binding and releasing, which eliminates a chemical reaction limit in the permeation behavior and enables a simple analysis of the permeation data, (ii) spectroscopic and electrochemical activity, which provides the oxygen-binding constants and the diffusion coefficient, independent of the permeation experiment, and (iii) sufficient lifetime as a reversible oxygen carrier, which makes the permeation experiment possible at ambient temperature and realizes a more feasible membrane. This paper describes by using the liquid membrane holding the cobalt porphyrin derivative (Chart 1) both an attempt to display important data for the oxygen permeability and oxygen/nitrogen permselectivity under practical conditions and an analysis of the facilitated oxygen transport in the liquid membrane holding an oxygen-carrying metal complex with the combination of permeation, spectroscopic, and electrochemical measurements.

† CREST Investigator, JST.

[®] Abstract published in *Advance ACS Abstracts*, July 1, 1997.

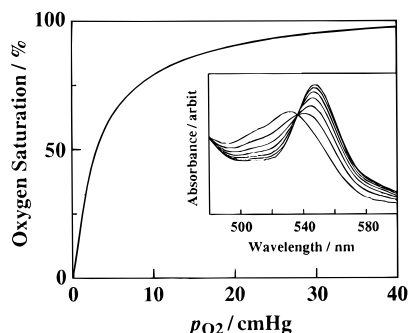
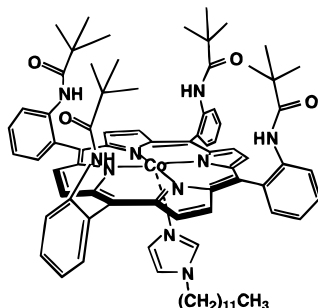


Figure 1. Oxygen-binding equilibrium curve for the cobalt porphyrin in the methylanisole solution at 10 °C. Inset: visible absorption spectra of the oxy and deoxy cobalt porphyrin.

CHART 1



Experimental Section

Materials and Membrane Preparation. [*meso*- $\alpha,\alpha,\alpha,\alpha$ -Tetrakis(*o*-pivalamidophenyl)porphyrinato]cobalt(II) (CoP) was synthesized as in the literature.¹⁰ The liquid membrane of CoP was prepared by immersing a three-layer microporous flat membrane made from polypropylene and polyethylene (Celgard 3501; Hoechst Celanese Co.; pore dimensions, $0.05 \times 0.19 \mu\text{m}$; porosity, 0.45; thickness, $25 \mu\text{m}$) into a 4-methylanisole solution of CoP with laurylimidazole as an axial ligand. The pores of the film were filled with the CoP solution by capillary action.

Results and Discussion

First, the carrier complex has a good solubility in order to be present at a high concentration in the liquid medium; both the carrier complex and the liquid medium clearly need to be nonvolatile during the air passage. *N*-Laurylimidazole and 4-methylanisole were selected as the axial ligand of CoP (Chart 1) and the liquid medium, respectively.

The oxygen-binding equilibrium curve or oxygen-saturation curve for the CoP complex in the methylanisole solution was spectroscopically measured on the same CoP solution used in the following membrane permeation. The visible absorption spectrum ($\lambda_{\text{max}} = 532 \text{ nm}$) of the deoxy CoP was reversibly changed to the spectrum ($\lambda_{\text{max}} = 548 \text{ nm}$) of oxy CoP with isosbestic points at 480, 537, and 667 nm, in response to the oxygen partial pressure in the atmosphere at -5 to 25 °C (inset in Figure 1). The equilibrium curve (Figure 1) indicates CoP acts as a reversible oxygen-binding carrier and obeys a Langmuir isotherm. The latter gave both the effective CoP fraction as the carrier and the oxygen-binding affinity or equilibrium constant of the oxygen-binding reaction (K in eq 1).

The effective CoP fraction in the solution was 0.99 ± 0.01 and was almost equal to the feed CoP concentration in the membrane liquid ($[\text{CoP}]_0$). The effective CoP fraction slowly decreased with time passage: Co(II)P was irreversibly oxidized to the inactive Co(III)P derivative during the repeated oxygen-

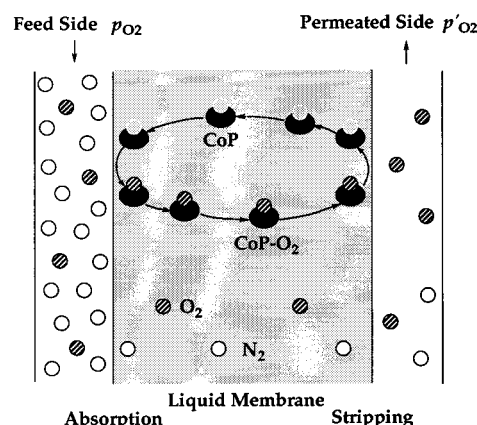


Figure 2. Schematic diagram of facilitated oxygen transport through the cobalt porphyrin liquid membrane.

binding reaction. The half-life of the CoP complex in the 4-methylanisole solution was 3 weeks and 10 days at -5 and 10 °C, respectively.¹¹

The binding equilibrium constant $K = 0.31 \text{ cmHg}^{-1}$ at 10 °C corresponds to the oxygen-binding affinity p_{50} (oxygen partial pressure to give a half-saturation of the binding site) = 3.2 cmHg . This supports the fact that CoP possesses a desirable oxygen-binding affinity as a carrier for the operation between an atmospheric feed stream and a permeated stream with reduced oxygen pressure. Enthalpy and entropy changes for the oxygen binding were estimated from the temperature dependency of K (van't Hoff plot) to be $-13 \text{ kcal mol}^{-1}$ and -41 eu , respectively, which were consistent with the previous reported values for the CoP complexed with 2-methylimidazole in toluene.^{10,12} They also indicate a stronger oxygen-binding affinity at lower temperature, e.g. $K = 0.99 \text{ cmHg}^{-1}$ at -5 °C.



Oxygen-binding and -releasing rate constants, k_{on} and k_{off} in eq 1, respectively, were estimated by pseudo-first-order kinetics on the spectral time courses for the oxygen recombination after a flash photolysis; $k_{\text{on}} = 4.8 \times 10^8 \text{ L mol}^{-1} \text{ s}^{-1}$ and $k_{\text{off}} = 2.9 \times 10^5 \text{ s}^{-1}$ at 20 °C mean that the CoP in the methylanisole solution is kinetically active in the oxygen-binding and -releasing reaction, as has been reported for the CoP complexed with 2-methylimidazole in toluene,^{10,12} and eliminates a chemical reaction-limiting process in the following permeation experiment.

Permeation across the CoP liquid membrane contains a specific transport mediated with the oxygen mobile carrier CoP in addition to physical dissolution-diffusion transport, as schematically represented in Figure 2. The liquid membrane separates the feed stream side from the permeated or product stream side. The oxygen carrier specifically combines with oxygen at the feed stream-membrane interface and converts it to the oxy form. The permeated stream is kept at a sufficiently low oxygen pressure (here with flowing inert helium gas) to strip oxygen or maintain the carrier in its deoxy form at the membrane-permeated stream interface. The oxygen carrier thus acts as a shuttle in response to the concentration gradients of its oxy and deoxy forms, picking up oxygen at the feed stream-membrane interface, diffusing across the membrane as the oxy form, releasing oxygen to the permeated stream, and the diffusing back to the feed stream-membrane interface to repeat the process. Because the carrier is specific for oxygen, the rate of oxygen transport is enhanced with no effect on the rate of

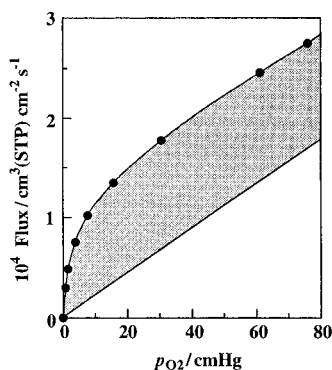


Figure 3. Oxygen simple flux (lower solid line) for the control membrane and the facilitated oxygen flux (plots) for the liquid membrane holding 31 wt % CoP, and 10 °C.

nitrogen transport, resulting in a considerably higher permeability of oxygen and higher selectivity of oxygen/nitrogen.

The oxy CoP concentration $[\text{CoPO}_2]$ in the liquid membrane is represented as in eq 2

$$[\text{CoPO}_2] = \frac{[\text{CoP}]_0 K p_{\text{O}_2}}{1 + K p_{\text{O}_2}} \quad (2)$$

Here, $[\text{CoP}]_0$ and p_{O_2} are the total CoP concentration in the liquid membrane and oxygen partial pressure at the feed stream, respectively. The permeability coefficient of oxygen ($\text{cm}^3(\text{STP}) \text{ cm cm}^{-2} \text{ s}^{-1} \text{ cmHg}^{-1}$) is defined as the product of the diffusivity and the solubility in a liquid membrane, which is often represented for the facilitated transport as a dual-mode permeation,^{13,14} according to the scheme in Figure 2.

$$P_{\text{O}_2} = k D_{\text{O}_2} + \frac{[\text{CoP}]_0 K D_{\text{CoP}}}{1 + K p_{\text{O}_2}} \quad (3)$$

Here, D_{CoP} , D_{O_2} , and k are the diffusion coefficient of CoP ($\text{cm}^2 \text{ s}^{-1}$), physical diffusion coefficient of oxygen ($\text{cm}^2 \text{ s}^{-1}$), and solubility of oxygen ($\text{cm}^3(\text{STP}) \text{ cm}^{-3} \text{ cmHg}^{-1}$) in the membrane solution, respectively. Because D_{CoP} , D_{O_2} , and k are constants at a given temperature and CoP concentration, P_{O_2} steeply increases with the decrease in p_{O_2} . The P_{O_2} increase at low p_{O_2} is expected to be enhanced at lower temperature, because K increases at lower temperature.

A typical result of oxygen flux through the CoP liquid membrane by two pathways is shown in Figure 3. The solid line represents the oxygen flux for the control liquid membrane containing the inactive Co(III)P derivative or the flux of physical dissolution–diffusion permeation which is proportional to the partial pressure difference of oxygen across the membranes. The closed symbols represent the total flux of oxygen (involving the facilitated flux) across the CoP membranes. The partial flux over the solid line (the shaded area in Figure 3) is ascribed to the oxygen flux of CoP-mediated or -facilitated transport; it steeply increases at low oxygen partial pressure and is predominant against the physical flux, and it becomes a constant at higher oxygen partial pressure of the feed stream (p_{O_2}). This flux curve of facilitated transport (the shaded area curve in Figure 3) corresponds to the oxygen-binding curve in Figure 1, which also supports the contribution of CoP as the oxygen carrier.

From eq 3 the facilitated flux (J_{CoP}) is represented as

$$J_{\text{CoP}} = \frac{[\text{CoP}]_0 K D_{\text{CoP}} p_{\text{O}_2}}{1 + K p_{\text{O}_2} l} \quad (4)$$

When p_{O_2} is large enough, the expression is derived as a

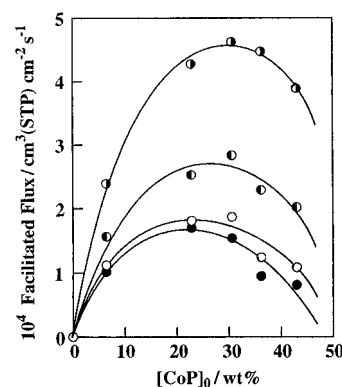


Figure 4. Effect of the cobalt porphyrin concentration in the liquid membrane $[\text{CoP}]_0$ on the facilitated oxygen flux through the membrane at (●) 25, (○) 10, (□) 0, and (●) −5 °C.

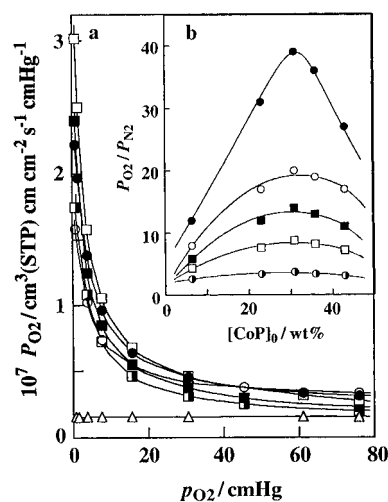


Figure 5. Effect of upstream oxygen pressure (p_{O_2}) on the oxygen permeation coefficient (P_{O_2}) through the cobalt porphyrin liquid membrane (a) and effect of the cobalt porphyrin concentration ($[\text{CoP}]_0$) on the permselectivity $P_{\text{O}_2}/P_{\text{N}_2}$ (b). $[\text{CoP}]_0$ in (a): (○) 6.4, (●) 23, (□) 31, (■) 36, (▣) 43 wt %. (Δ) CoP(III)P control 31 wt %. p_{O_2} in (b): (●) 0.8, (○) 3.8, (■) 7.6, (□) 15.7, (●) 76 cmHg, at 10 °C.

constant:

$$J_{\text{CoP}} = \frac{[\text{CoP}]_0 D_{\text{CoP}}}{l} \quad (5)$$

Thus, the value of J_{CoP} is determined by $[\text{CoP}]_0$, D_{CoP} , and l (the thickness of the membrane).

The relationship between J_{CoP} , the CoP concentration in the membrane $[\text{CoP}]_0$, and the measurement temperature is shown in Figure 4. J_{CoP} was enhanced to a maximum at $[\text{CoP}]_0 = 31$ wt % at 25 °C and decreased with increasing $[\text{CoP}]_0$ beyond the maximum. The $[\text{CoP}]_0$ value to yield the maximum decreases at lower temperature; $[\text{CoP}]_0 = 23$ wt % at −5 °C. This is because the D_{CoP} value decreases with $[\text{CoP}]_0$, probably due to the viscosity of the solution, and increases with temperature.

Figures 5 and 6 are examples to show the effect of feed stream oxygen pressure (p_{O_2}) on the permeability coefficient of oxygen (P_{O_2}) and the oxygen/nitrogen permselectivity through the CoP liquid membranes. The oxygen permeability significantly increased with a decrease in p_{O_2} , as seen in Figures 5a and 6a. The steep increase in P_{O_2} or the facilitation effect at low p_{O_2} was enhanced at lower temperatures, as shown in Figure 6, while P_{O_2} itself decreased at lower temperature due to the decrease in diffusivity. On the other hand, P_{O_2} for the control and inactive Co(III)P membrane was lower than that for the

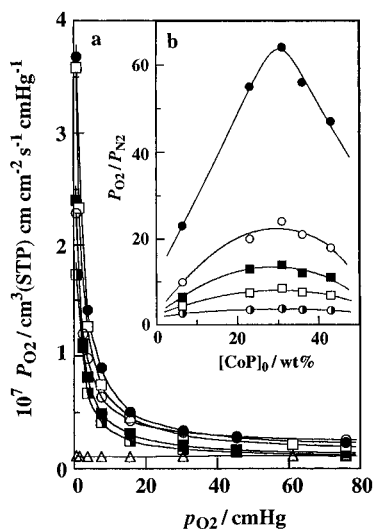


Figure 6. Effect of upstream oxygen pressure (p_{O_2}) on the oxygen permeation coefficient (P_{O_2}) through the cobalt porphyrin liquid membrane (a) and effect of the cobalt porphyrin concentration ($[\text{CoP}]_0$) on the permselectivity P_{O_2}/P_{N_2} (b). $[\text{CoP}]_0$ in (a): (○) 6.4, (●) 23, (□) 31, (■) 36, (▨) 43 wt %. (△) CoP(III)P control 31 wt %. P_{O_2} in (b): (●) 0.8, (○) 3.8, (■) 7.6, (□) 15.7, (●) 76 cmHg, at -5°C .

corresponding active membrane, was independent of p_{O_2} , and was not enhanced at the low p_{O_2} . These permeation behaviors are in accordance with the carrier-mediated or -facilitated transport in this liquid membrane, which supports the following analysis using a dual-mode transport model, as represented by eq 3.

Figures 5b and 6b show that the permselectivity, P_{O_2}/P_{N_2} , obviously increases with the CoP carrier concentration and reaches a maximum at around $[\text{CoP}]_0 = 31 \text{ wt} \%$. Oxygen/nitrogen permselectivity, P_{O_2}/P_{N_2} , and the facilitation factor (the ratio of P_{O_2} at low p_{O_2} (here $p_{O_2} = 0.8 \text{ cmHg}$) to P_{O_2} at higher p_{O_2} (here $p_{O_2} = 76 \text{ cmHg}$) became more than 60 and 30, respectively, for the membrane of 31 wt % CoP, at -5°C and $p_{O_2} = 0.8 \text{ cmHg}$, and still at 8 and 4, at $p_{O_2} = 15.7 \text{ cmHg}$ (the same p_{O_2} as in air) (see Figure 6). Because both P_{O_2} and P_{N_2} increase with temperature due to the increase in the diffusivity of oxygen and nitrogen, the permselectivity, P_{O_2}/P_{N_2} , decreases with temperature. However, even at 10°C (see Figure 5), the 31 wt % CoP membrane displayed a $P_{O_2}/P_{N_2} = 40$ and the facilitation factor = 20.

The facilitated transport data (P_{O_2} at various p_{O_2} , $[\text{CoP}]_0$, and at any temperature) were appropriately analyzed in terms of the dual-mode transport model (represented by eq 3). P_{O_2} was plotted versus $[\text{CoP}]_0 K / (1 + K p_{O_2})$, as shown using the example of the 31 wt % CoP membrane in Figure 7. The linear relationship at any $[\text{CoP}]_0$ and any measurement temperature supports the validity of the analysis using the dual-mode transport model.

The diffusion coefficient (D_{CoP}) of CoP through the membrane was estimated from the slope of the linear relationship in Figure 7. D_{CoP} at various $[\text{CoP}]_0$'s is shown in Figure 8. D_{CoP} is almost on the order of $10^{-7} \text{ cm}^2 \text{ s}^{-1}$ and decreases with the increase in $[\text{CoP}]_0$ probably due to the viscosity of the CoP solution. The latter supports the role of CoP as a mobile carrier in the membrane.

The diffusion coefficient of CoP in the methylanisole solution was also evaluated by an electrochemical method. Levich plots (inset in Figure 8) for the anodic plateau currents gave the diffusion coefficient of $1.7 \times 10^{-6} \text{ cm}^2 \text{ s}^{-1}$ for CoP. This diffusion of CoP corresponds to D_{CoP} in a dilute solution and is comparable with the D_{CoP} at 25°C estimated with the analysis

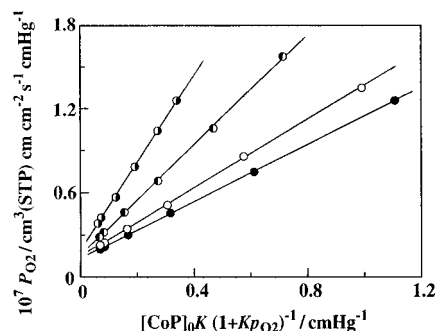


Figure 7. Calculation of permeation coefficient (kD_{O_2}) and diffusion coefficient mediated with the cobalt porphyrin (D_{CoP}) from the dual-mode model. $[\text{CoP}]_0 = 31 \text{ wt} \%$, at (●) 25, (○) 10, (○) 0, and (●) -5°C .

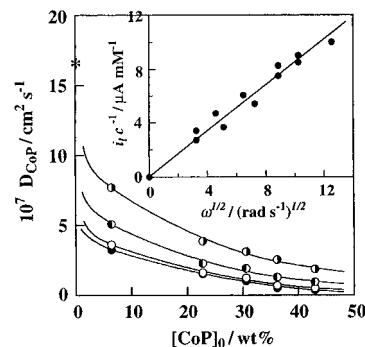


Figure 8. Diffusion coefficient of cobalt porphyrin (D_{CoP}) in the liquid membrane at (●) 25, (○) 10, (○) 0, and (●) -5°C . *: diffusion coefficient determined from the Levich plots at 25°C . Inset: Levich plots of the cobalt porphyrin in methylanisole at 25°C .

of permeation data. The fairly good agreement between the two values not only supports the analysis based on the dual-mode transport model but also provides evidence that CoP acts as a mobile carrier in the membrane.

The permeability of oxygen for the physical diffusion transport (kD_{O_2} : the first term in eq 2) in the CoP liquid membrane was estimated from the intercept of the linear relationship in Figure 7. The physical permeability decreases with $[\text{CoP}]_0$ at every temperature. Oxygen solubility in the methylanisole portion in the membranes at any $[\text{CoP}]_0$ was calculated under the following assumption.

$$k = k'(100 - [\text{CoP}]/\rho_{\text{CoP}})/100 \quad (6)$$

where ρ_{CoP} and k' are the density of CoP in the solid state and the oxygen solubility of pure methylanisole at the different temperature, respectively. $\rho_{\text{CoP}} = 1.7 \text{ g cm}^{-3}$ and k' for oxygen and nitrogen = 1.8×10^{-3} and $1.0 \times 10^{-3} \text{ cm}^3 (\text{STP}) \text{ cm}^{-3} \text{ cmHg}^{-1}$, respectively, (both measured in this experiment) and were substituted into eqs 3 and 6 to give the diffusion constant of oxygen in the membrane, D_{O_2} (Figure 9). D_{O_2} is almost on the order of $10^{-5} \text{ cm}^2 \text{ s}^{-1}$ and slightly decreases with $[\text{CoP}]_0$.

The diffusion coefficient of the CoP carrier, D_{CoP} , was 100 times smaller than the physical diffusion coefficient of oxygen, D_{O_2} , in the same membrane. On the other hand, the chemically specific solubility of oxygen ascribed to CoP ($[\text{CoP}]_0 K / (1 + K p_{O_2}) = 7.0 \times 10^{-2} \text{ cm}^3 (\text{STP}) \text{ cm}^{-3} \text{ cmHg}^{-1}$) yields a 50 times enhancement in the oxygen solubility in comparison with the physical solubility of oxygen, at the feed stream oxygen partial pressure of $p_{O_2} = 76 \text{ cmHg}$. Furthermore, this chemical specific oxygen solubility becomes 3000 times greater than the physical solubility at $p_{O_2} = 0.8 \text{ cmHg}$. This extraordinarily larger solubility of oxygen in the membrane contributes to the

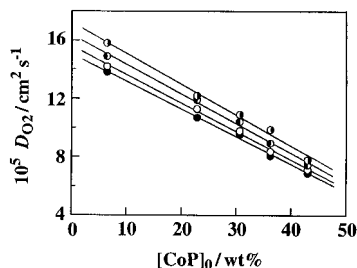


Figure 9. Diffusion coefficient of oxygen (D_{O_2}) in the methylanisole liquid membrane at (○) 25, (◐) 10, (○) 0, and (●) -5 °C.

enhanced oxygen permeability and oxygen/nitrogen permselectivity shown in Figures 5 and 6.

The authors previously examined facilitated oxygen transport through a solid or solvent-free polymer membrane that held the same CoP as a fixed oxygen carrier.^{2,9a} The CoP solid membrane was in use for a long period of time (half-life > 3 months) at room temperature. The CoP liquid membrane in this paper displayed both high permeability and permselectivity, in spite of unresolved issues such as the chemical instability of the CoP carrier in the solution, the evaporation loss of the liquid medium, and the resulting operational range being restricted to low temperatures. While high permeability was sacrificed in order to yield the oxygen flux, due to the unavoidable membrane thickness of the liquid membrane, oxygen/nitrogen permselectivity was more than 60 and 40 for the 31 wt % CoP liquid membrane at -5 and 10 °C, respectively. This facilitated and chemically specific effect could be attributed to the enormous enhancement in the oxygen solubility into the membrane (in the above discussion). The advantage of using a liquid membrane in comparison with a solid membrane was the high solubility of the carrier CoP in the membrane without any heterogeneous distributions and pin holes. This was demonstrated in this paper by a combination of the CoP species in Chart 1 and the methylanisole medium.

Acknowledgment. This work was partially supported by a Grant-in-Aid for Scientific Research from the Ministry of Education, Science, Sports, and Culture, Japan. X.S.C. thanks the Monbusho for a Scholarship which supported his stay in Japan.

Supporting Information Available: Permeation measurement, spectroscopic measurements, and electrochemical diffusion coefficient measurement (2 pages). See any current masthead page for ordering and internet access instructions.

References and Notes

- (1) Way, J. D.; Noble, R. D. In *Membrane Handbook*; Winston Ho, W. S., Sirkar, K. K., Eds.; van Nostrand Reinhold: New York, 1993; Chapter 44, pp 833–866.
- (2) Nishide, H.; Tsuchida, E. In *Polymers for Gas Separation*; Toshima, N., Ed.; VCH Publishers: New York, 1992; Chapter 6, pp 183–219.
- (3) Scholander, P. F. *Science* **1960**, *131*, 585.
- (4) Chen, X. S.; Nishide, H.; Tsuchida, E. *Bull. Chem. Soc. Jpn.* **1996**, *69*, 255.
- (5) (a) Roman, I. C.; Baker, R. W. U.S. Patent 4,542,010, 1985. (b) Johnson, B. M.; Baker, R. W.; Matson, S. L.; Smith, K. L.; Roman, I. C.; Tuttle, M. E.; Lonsdale, H. K. *J. Membr. Sci.* **1987**, *31*, 31.
- (6) Tsuchida, E.; Nishide, H. *Top. Curr. Chem.* **1986**, *132*, 63.
- (7) Tsuchida, E. Ed.; *Artificial Red Cells*; John Wiley: New York, 1995.
- (8) Tsuchida, E. Ed.; *Macromolecular Complexes*; VCH Publishers: New York, 1991.
- (9) (a) Nishide, H.; Ohyanagi, M.; Okada, O.; Tsuchida, E. *Macromolecules* **1987**, *20*, 417. (b) Nishide, H.; Kawakami, H.; Kurimura, Y.; Tsuchida, E. *J. Am. Chem. Soc.* **1989**, *111*, 7175. (c) Nishide, H.; Suzuki, T.; Nakagawa, R.; Tsuchida, E. *J. Am. Chem. Soc.* **1994**, *45*, 3261.
- (10) Collman, J. P.; Gagne, R. R.; Reed, C. A.; Halbert, J. R.; Lang, G. W.; Robinson, T. *J. Am. Chem. Soc.* **1975**, *97*, 1427.
- (11) The following permeation experiments (10 experiments for one membrane) were carried out within 8 h after the membrane preparation, and the effective CoP fraction was spectroscopically checked to be >0.95 after each experiment.
- (12) Tsuchida, E.; Nishide, H.; Ohyanagi, M.; Okada, O. *J. Phys. Chem.* **1988**, *92*, 6461.
- (13) Paul, D. R.; Koros, W. J. *J. Polym. Sci., Polym. Phys. Ed.* **1976**, *14*, 675.
- (14) Barrer, R. M. *J. Membr. Sci.* **1984**, *18*, 25.